IOPscience iopscience.iop.org

Home Search Collections Journals About Contact us My IOPscience

The cumulant expansion of the periodic Anderson model; completeness and the Φ-derivable approximation

This article has been downloaded from IOPscience. Please scroll down to see the full text article.

1996 J. Phys.: Condens. Matter 8 5017

(http://iopscience.iop.org/0953-8984/8/27/012)

View the table of contents for this issue, or go to the journal homepage for more

Download details:
IP Address: 171.66.16.206
The article was downloaded on 13/05/2010 at 18:17

Please note that terms and conditions apply.

J. Phys.: Condens. Matter **8** (1996) 5017–5038. Printed in the UK

The cumulant expansion of the periodic Anderson model; completeness and the Φ-derivable approximation

M S Figueira† and M E Foglio‡

† Instituto de Física, CP 100.093, Universidade Federal Fluminense, UFF, 24001-970 Niterói, Rio de Janeiro, Brazil

‡ Instituto de Física 'Gleb Wataghin', Universidade Estadual de Campinas, UNICAMP, 13083-970 Campinas, São Paulo, Brazil

Received 15 December 1995, in final form 4 March 1996

Abstract. The approximate Green's functions of the localized electrons, obtained by the cumulant expansion of the periodic Anderson model in the limit of infinite Coulomb repulsion, do not satisfy completeness even for the simplest families of diagrams, like the chain approximation. The idea that employing Φ-derivable approximations would solve this difficulty is shown to be false by proving that the chain approximation is Φ-derivable and does not satisfy completeness. After finding a family of diagrams with Green's functions that satisfy completeness, we put forward a conjecture that shows how to select families of diagrams with this property.

1. Introduction

The cumulant expansion that was employed by Hubbard [1] to study a model of a strongly correlated system, currently known as the 'Hubbard model' [2], was extended to the periodic Anderson model (PAM) in a previous paper [3] (which in the following will be referred to as I). The method employed by Hubbard was a perturbative expansion around the atomic limit. He introduced the operators $X_{j,ab} = |j,b\rangle\langle j,a|$ that transform the local state $|a\rangle$ at site j into the local state $|b\rangle$ at the same site. He developed a diagrammatic method that circumvents the fact that the X-operators do not satisfy the usual commutation properties of the fermion or boson operators, obtaining a linked cluster expansion that involves unrestricted lattice sums of connected diagrams [4, 5]. Hubbard's method [1] has been applied to the PAM by Hewson [6], and the rules for the diagrammatic expansion in real space and imaginary time, as well as those for reciprocal space and frequencies, were explicitly derived in I. Both the hopping of the conduction electrons and the intra-site Coulomb repulsion U between the localized or f electrons were included in the unperturbed Hamiltonian in I. A rectangular conduction band was employed, because it simplifies the analytic calculations while still showing the main features of the model. At a given site j, the state space of the f electrons is spanned by four states: the vacuum state $|j,0\rangle$, the two states $|j,\sigma\rangle$ of one f electron with spin component σ, and the state $|j,2\rangle$ with two electrons of opposite spin. The PAM in the limit of infinite electronic repulsion ($U = \infty$) is considered in the present paper, so that the state $|j,2\rangle$ is always empty, and can be projected out of the space. In this reduced space, the identity I_j at site j should satisfy the completeness relation:

$$X_{j,00} + X_{j,\sigma\sigma} + X_{j,\bar{\sigma}\bar{\sigma}} = I_j \tag{1.1}$$

0953-8984/96/275017+22$19.50 © 1996 IOP Publishing Ltd

where $\bar{\sigma}$ is the spin component opposite to σ, and the three $X_{j,aa}$ are projectors into the three states $|j,0\rangle$ and $|j,\sigma\rangle$ of the basis. The statistical averages n_a of $X_{j,aa}$ are independent of j because of translational invariance, and can be calculated from the approximate Green's functions (GF). From equation (1.1) it should follow that

$$n_0 + n_\sigma + n_{\bar{\sigma}} = 1. \tag{1.2}$$

It was shown in I that this relation (called 'completeness' in what follows) is not satisfied in general, and in particular that it fails for the well known chain approximation (CHA) [6, 7, 8], which is the more general cumulant expansion with only second-order cumulants. The purpose of this paper is to discuss this basic problem of the cumulant expansion, and to propose a systematic way of adding a set of diagrams to an arbitrary family so that completeness is satisfied by the n_a calculated with the corresponding approximate GF.

Our first attempt to solve this problem was to employ the Φ-derivable approximations (cf. Wortis [4]) that were introduced in a different context by Baym and Kadanoff [9] under the name of 'conservative approximations'. For the cumulant expansions, they are obtained by starting from a family of 'skeleton diagrams' [4] and decorating the vertices in all of the possible different manners. The order of the cumulants that appear in the corresponding contributions increases with the added decorations, so a full calculation becomes impractical because of the difficulty of calculating higher-order cumulants; one should then resort to keeping only cumulants up to a small order (fourth in our case). The failure of these approximations to satisfy completeness could then be attributed to the truncation of the family of diagrams. This situation was clarified when we found that the CHA is a Φ-derivable approximation without any truncation of the family of diagrams, and this type of Φ-derivable approximation will be called 'exact' in what follows. The fact that the CHA does not satisfy completeness shows that employing Φ-derivable approximations does not guarantee that property, and that a different type of solution should be pursued.

The main result of the present paper is to show how to add diagrams to the GF in the CHA, so that the increased family satisfies completeness. This leads us to state a conjecture that gives a systematic way of achieving completeness by adding a set of diagrams to an arbitrary family. This conjecture has been verified in a number of cases, including diagrams with infinite fourth-order cumulants, but a general derivation has not yet been found. A family of diagrams built following this conjecture will be called a 'complete-cumulant approximation' (CCA). From the stated conjecture it naturally follows that the approximate GF for the conduction electrons do not require the addition of extra diagrams to satisfy completeness.

2. Some basic aspects of the PAM

2.1. The Hamiltonian and the Hubbard operators

The perturbative treatment of the electronic Coulomb repulsion leads to singularities caused by the long range of this interaction, and summation of an infinite series of the most divergent terms is necessary to remove them. To study the problem from an atomic point of view, Hubbard considered the most important local contribution in this limit, describing the interaction at each site j by the term $Un_{j\uparrow}n_{j\downarrow}$, where the $n_{j\sigma}$ is the number operator of an electron localized at site j with spin component σ. In Hubbard's model the electrons can jump between sites, and the problem remains rather difficult to treat, even with the removal of the long-range interaction.

In the PAM, two types of electronic state are considered: (i) localized electrons with the

interaction $Un_{j\uparrow}n_{j\downarrow}$, but without hopping; and (ii) a wide band of uncorrelated electrons. A hybridization term is also added, allowing electronic transitions between the two types of state and thus giving mobility to the f electrons. The PAM is considered to provide a good schematic description of systems like transition metal and rare-earth compounds, as well as intermediate-valence and heavy-fermion systems.

Employing Hubbard operators, the Hamiltonian of the PAM in the limit of infinite Coulomb repulsion ($U = \infty$) can be written as [3]

$$H = \sum_{\boldsymbol{k},\sigma} E_{\boldsymbol{k},\sigma} C^{\dagger}_{\boldsymbol{k},\sigma} C_{\boldsymbol{k},\sigma} + \sum_{j,\sigma} E_{j,\sigma} X_{j,\sigma\sigma} + H_h. \tag{2.1}$$

The first term of this equation corresponds to the uncorrelated conduction band, where the $C^{\dagger}_{\boldsymbol{k},\sigma}$ and $C_{\boldsymbol{k},\sigma}$ are the usual operators for creation and destruction of c electrons with wave vector $\boldsymbol{k}$, component σ of spin and energy $E_{\boldsymbol{k},\sigma}$ respectively. The second term describes the independent sites of f electrons, while the last term is the hybridization Hamiltonian, which is considered a perturbation in the present work:

$$H_h = \sum_{j,\boldsymbol{k},\sigma} (V_{j,\boldsymbol{k},\sigma} X^{\dagger}_{j,0\sigma} C_{\boldsymbol{k},\sigma} + V^{*}_{j,\boldsymbol{k},\sigma} C^{\dagger}_{\boldsymbol{k},\sigma} X_{j,0\sigma}). \tag{2.2}$$

The operator H acts on a space from which all the local states $|j, 2\rangle$, with two electrons of opposite spin at site j, have been projected out. The operator $X_{j,0\sigma}$ destroys the electron in state $|j, \sigma\rangle$ leaving the site in the vacuum state $|j, 0\rangle$ with energy $E_{j,0} = 0$, and its Hermitian conjugate $X^{\dagger}_{j,0\sigma} = X_{j,\sigma 0}$ reverses that process.

The U has disappeared from the Hamiltonian of equation (2.1) through the introduction of the $X_{j,ab}$, and it is the special properties of these operators that are now responsible for all the correlations due to the Coulomb interaction U.

The Hubbard operators $X_{j,ab}$ are not usually Fermi or Bose operators, and the product rule

$$X_{j,ab} X_{j,cd} = \delta_{bc} X_{j,ad} \tag{2.3}$$

should be employed when the two operators are at the same site. For different sites one should first classify the operators into two families: one says that $X_{j,ab}$ is of the 'Fermi type' when $|a\rangle$ and $|b\rangle$ differ by an odd number of fermions, and that it is of the 'Bose type' when they differ by an even number of fermions. The most convenient definition is then to say that at different sites, two X-operators of the Fermi type anticommute, and that they commute when at least one of them is of the Bose type. Clearly the $X^{\dagger}_{j,0\sigma}$ and $X_{j,0\sigma}$ are of the Fermi type, and the $X_{j,\sigma\sigma}$ and $X_{j,00}$ are of the Bose type. To complete the definition, the $X_{j,ab}$ should anticommute (commute) with the $C^{\dagger}_{\boldsymbol{k},\sigma}$ and $C_{\boldsymbol{k},\sigma}$ when they are of the Fermi type (Bose type).

As the grand canonical ensemble of electrons is employed, the Hamiltonian H in the statistical operator is substituted for with

$$\mathcal{H} = H - \mu\left(\sum_{\boldsymbol{k},\sigma} C^{\dagger}_{\boldsymbol{k},\sigma} C_{\boldsymbol{k},\sigma} + \sum_{j,a} \nu_a X_{j,aa}\right) = \mathcal{H}_0 + H_h \tag{2.4}$$

where ν_a is the number of electrons in state $|a\rangle$ and μ is the electronic chemical potential. Most formulas then look simpler when the shifted energies

$$\epsilon_{j,a} = E_{j,a} - \nu_a \mu \qquad \text{and} \qquad \epsilon_{\boldsymbol{k},\sigma} = E_{\boldsymbol{k},\sigma} - \mu \tag{2.5}$$

are employed.

The symbols Y_γ and $Y(\gamma)$ will be used in the following sections to denote both the X- and C-operators, where γ includes all of the indices necessary to characterize the operator.

For the X-operators $\gamma = (f; j, \alpha, u)$, where j is the site and α identifies the transition $|a\rangle \rightarrow |b\rangle$ with the restriction that $|a\rangle$ has just one electron more than $|b\rangle$, and $u = \pm$, so $Y_\gamma = X_{j,ba}$ for $\gamma = (f; j, \alpha, u = -)$ and $Y_\gamma = X^\dagger_{j,ba}$ for $\gamma = (f; j, \alpha, u = +)$. For the C-operators $Y_\gamma = C_{\boldsymbol{k},\sigma}$ for $\gamma = (c; \boldsymbol{k}, \sigma, u = -)$ and $Y_\gamma = C^\dagger_{\boldsymbol{k},\sigma}$ for $\gamma = (c; \boldsymbol{k}, \sigma, u = +)$. The operator Y_γ in the interaction and Heisenberg pictures will be denoted by $Y(\gamma, \tau)$ and $\widehat{Y}(\gamma, \tau)$ respectively, and $\langle A\rangle_{\mathcal{H}}$ and $\langle A\rangle$ will be respectively used for exact and unperturbed averages in the grand canonical ensemble.

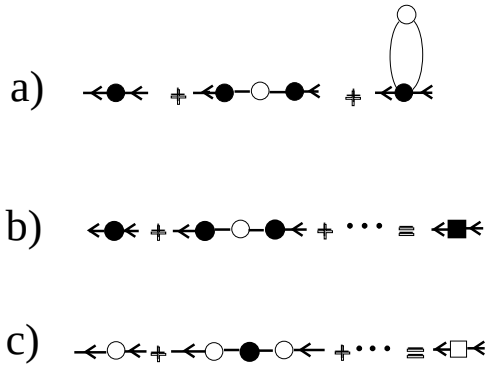

Figure 1. Typical cumulant diagrams for one-particle GF. (a) The simplest family of diagrams that satisfies completeness (cf. section 4). (b) The diagrams of the chain approximation for the f-electron GF, represented by the filled square to the right. (c) As (b), but for the c electrons, represented by an empty square.

2.2. The diagrammatic expansion for the PAM

The cumulant expansion employed in the present work [3] has been widely used for the classic Ising model [4] and extended to quantum fermionic systems by Hubbard [1]. Because the starting point is the atomic limit, the meaning of the diagrams is different from that of the widely used Feynman diagrams, and a brief description of this type of diagrammatic expansion therefore seems adequate. In I, the diagrammatic expansion for both the grand canonical potential and the GF are given in detail, but only the diagrams contributing to the GF of the type $\langle(\widehat{X}_{j,\alpha}(\tau)\widehat{X}_{j',\alpha'})_+\rangle_{\mathcal{H}}$ are considered here. Notice that the Matsubara expansion is employed, so τ is the imaginary time,

$$\widehat{X}_{j,\alpha}(\tau) = \exp(\tau\mathcal{H})X_{j,\alpha}\exp(-\tau\mathcal{H})$$

and the subscript $+$ indicates that the operators inside the parentheses are taken in the order of increasing τ to the left, with a change of sign when the two Fermi-type operators have to be exchanged to obtain this ordering.

In figure 1(a) we show three of the infinite diagrams that contribute to $\langle(\widehat{X}_{j,\alpha}(\tau)\widehat{X}_{j',\alpha'})_+\rangle_{\mathcal{H}}$. The full circles (f vertices) correspond to the cumulants [10] of the f electrons. Each line reaching a vertex is associated with one of the X-operators of the cumulant, and the free lines (not joining an empty circle) correspond to the external X-operators appearing in the exact GF. The f cumulants are linear combinations of products of free propagators, each term having a total number of X-operators equal to the order of the cumulant. The first diagram in figure 1(a) corresponds to the simplest free propagator $\langle(X_{j,\alpha}(\tau)X_{j',\alpha'})_+\rangle$, and the second diagram in that figure has an empty circle (c

vertex) that corresponds to the conduction electron cumulant, equal to the free propagator $\langle (C_{k\sigma}(\tau)C^{\dagger}_{k\sigma})_{+}\rangle$. The interaction is represented by the lines (edges) joining two vertices, and because of the structure of H_h they always join two different vertices; the number of edges in a diagram gives its order in the perturbation expansion. To explicitly define the cumulants, it is necessary to introduce external fields ξ in the Hamiltonian, by adding the extra term

$$H_e(\xi) = -\sum_{\gamma} \xi_{\gamma}(\tau) Y_{\tau} = H_e[\xi(\tau)]$$

to equation (2.4), which already depends on τ in the Schrödinger picture through the independent fields $\xi_{\gamma}(\tau)$. The ξ_{γ} are Grassmann variables, which anticommute between themselves and with all the Y_{τ} of the problem. Keeping non-zero ξ_{γ}, the nth-order cumulant is defined by

$$M^0_n(l_1, l_2, \ldots, l_n; \xi) \equiv \langle (Y(l_1)\cdots Y(l_n))_{+}\rangle^{\xi}_c = \delta_1\delta_2\cdots\delta_n \ln[\mathcal{Z}_0(\beta, \xi)] \tag{2.6}$$

where $\mathcal{Z}_0(\beta, \xi)$ is the unperturbed grand partition function (i.e., with all $V_{j,\boldsymbol{k},\sigma} = 0$) in the presence of ξ, and the symbol δ_a is used to indicate the functional derivative $(\delta/\delta\xi(l_a))$.

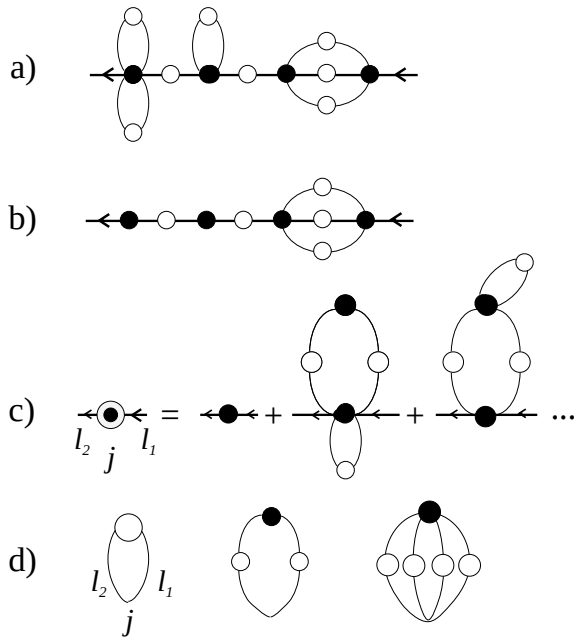

Figure 2. In (a) a linked diagram of the GF for $\xi = 0$ is shown, and in (b) its skeleton diagram is given. (c) A propagator with a renormalized local vertex (with $\xi = 0$) shown as a full circle inside a dashed circle, together with few of the unrenormalized diagrams it represents. (d) A few of the unrenormalized diagrams that constitute the self-field.

Cumulants containing statistically independent operators are zero, and those appearing in the present expansion (with H_h as a perturbation) vanish unless they contain only X-operators at the same site or only C- or $C^{\dagger}$-operators with the same k and σ. In the final expansion one sets $\xi_{\gamma} = 0$, and the only c cumulants left are of second order, because the uncorrelated C-operators satisfy Wick's theorem. On the other hand, the f vertices can have many legs, all corresponding to X-operators at the same site, like the fourth-order cumulant

appearing in the third diagram of figure 1(a). A rather more complicated diagram is shown in figure 2(a), showing a sixth-order cumulant.

The family of all of the infinite diagrams with cumulants of at most second order is shown in figure 1(b), and the corresponding family for the GF of the c electrons is shown in figure 1(c). Describing the full GF with this subfamily of all of the diagrams is called the 'chain approximation' (CHA), and it gives the exact solution when there is no Coulomb correlation ($U = 0$). When the spin is eliminated from the problem, the Hamiltonian of equation (2.1) has no correlation term and the CHA is again an exact solution. The meaning of the CHA will be further discussed in section 3.

In the Feynman perturbation expansion, Wick's theorem is valid and only second-order propagators appear, while the interactions are provided by the Coulomb interaction. In the present treatment the U has disappeared in the limit $U \to \infty$ (or is included in the unperturbed Hamiltonian when U is finite), and the correlations appear through the properties of the X-operators, because they have non-zero cumulants of order higher than two, that include propagators for two and more particles. In the Feynman expansion of the one-particle GF, the two-particle GF appear in the self-energy, which contains all of the correlations.

2.3. Calculation of the electronic occupation numbers

To calculate the f-electron occupation numbers one should employ the exact GF in real space and imaginary time τ, which can be related to the corresponding GF in reciprocal space and frequency by (cf. equation (3.31) in I)

$$\left\langle (\widehat{Y}(f;j,0\sigma,u,\tau)\widehat{Y}(f;j',0\sigma,u',\tau'))_+ \right\rangle_{\mathcal{H}} = \frac{1}{\beta N_s}\sum_{\boldsymbol{k},k'}\sum_{\omega\omega'} \exp[-\mathrm{i}(u\boldsymbol{k}\cdot\boldsymbol{R}_j + u'\boldsymbol{k}'\cdot\boldsymbol{R}'_j) - \mathrm{i}(\omega\tau + \omega'\tau')] \left\langle (\widehat{Y}(f;\boldsymbol{k},o\sigma,u,\omega)\widehat{Y}(f;\boldsymbol{k}',o\sigma,u',\omega'))_+ \right\rangle_{\mathcal{H}} \tag{2.7}$$

where $\boldsymbol{R}_j$ is the position of site j. A similar expression is obtained for the c-electron GF by employing the transformation of the operators $C_{\boldsymbol{k},\sigma}$ to the Wannier representation. Because of the invariance under lattice and time translations it follows that

$$\langle (\widehat{Y}(f;\boldsymbol{k}_2,\alpha_2,u_2=-,\omega_2)\widehat{Y}(f;\boldsymbol{k}_1,\alpha_1,u_1,\omega_1))_+ \rangle_{\mathcal{H}} \equiv G^{ff}_{\alpha_2\alpha_1}(\boldsymbol{k}_2,\omega_2)\Delta(u_2\boldsymbol{k}_2 + u_1\boldsymbol{k}_1)\Delta(u_2+u_1)\Delta(\omega_2+\omega_1). \tag{2.8}$$

In the usual way [11], one assigns the values $G^{ff}_{\sigma\sigma'}(\boldsymbol{k},\omega)$ to the points $\mathrm{i}\pi\nu/\beta$ along the imaginary axis of the complex frequency $z = \omega + \mathrm{i}y$ (where ω is a real energy variable already shifted by μ as discussed in section 2.1), and makes the analytic continuation to the upper and lower half-planes of the complex frequency z. The resulting function $\bar{G}^{ff}_{\sigma\sigma'}(\boldsymbol{k},z)$ is minus the Fourier transform of the real-time GF, and many properties of the system can be calculated with these GF. Usually one has to integrate $\bar{G}^{ff}_{\sigma\sigma'}(\boldsymbol{k},z)$ times a function of z along a circuit very close to the real axis in the complex plane. In the paramagnetic case one finds

$$n_f = \int_{-\infty}^{\infty} \rho_f(\omega) f_T(\omega)\ \mathrm{d}\omega \tag{2.9}$$

$$n_0 = \int_{-\infty}^{\infty} \rho_f(\omega)(1 - f_T(\omega))\ \mathrm{d}\omega \tag{2.10}$$

where

$$\rho_f(\omega) = \frac{1}{\pi}\lim_{\epsilon\to 0}\mathrm{Im}\left\{\frac{1}{N_s}\sum_{\boldsymbol{k}}\bar{G}^{ff}_{\sigma\sigma'}(\boldsymbol{k},\omega+\mathrm{i}\epsilon)\right\} \tag{2.11}$$

is the total spectral density of the f electrons per site and per spin component.

3. The chain approximation as a Φ-derivable approximation

The Φ-derivable approximation was introduced by Baym and Kadanoff [9] for a system with two-particle interactions, and a review of its application to the Ising model was given by Wortis [4]. The related vertex renormalization was recently discussed by Metzner [5] for the cumulant expansion of the Hubbard model, and its general treatment is closely related to ours, so only a rather brief discussion of the method will be presented here.

In this method one represents the whole family of diagrams that give the exact GF with a family of 'skeleton' diagrams [4], in which the local vertices have no 'insertions' [4] (cf. figure 2(b), which shows the skeleton diagram of figure 2(a)). This is accomplished by replacing each bare cumulant M_n^0 at a local vertex in the skeleton diagrams with the renormalized M_n (cf. figure 2(c)), which includes the contribution of all of the possible insertions at the same vertex (the subscript n indicates the number of edges reaching that vertex in the skeleton diagram).

The insertions are represented by diagrams in which the 'external vertex' [4] (i.e., the one belonging to the skeleton diagram) is left without the full or empty circle (cf. figure 2(d)). Its contribution is calculated in the same way as for the corresponding GF diagrams (cf. rules 3.5–6 in I), but replacing the cumulant at the external vertex by the number 1. It is convenient to classify the insertions by their 'valence' [4], i.e. the number of edges reaching to the external vertex, and each of these edges is associated with one operator $Y(l) = Y_\gamma(\tau)$, which would appear in the cumulant corresponding to that vertex in the full diagram. The index $l = (\gamma, \tau)$ characterizes completely the operator $Y(l)$, and is kept fixed in the definition of the insertion diagram.

To obtain M_n it is convenient to introduce the 'self-field' [4] $S_m(l_1, l_2, \ldots, l_m)$, which gives the sum of the contributions of all the topologically distinct and connected insertions, with m external edges associated with the indices $l_1, l_2, \ldots, l_m$ (a connected insertion is one that does not split when its external edges are separated at the external vertex).

The Grassmann external fields ξ introduced in I must be kept in the M_n and S_m in order to use the equation (2.6) (cf. equation (3.14) in I). Even in the presence of ξ, the $M_n^0(l_1, l_2, \ldots, l_m; \xi)$ are zero [3, 4] unless either all the $l_1, l_2, \ldots, l_m$ correspond to 'local' $Y(l)$ at the same site j or all correspond to 'conduction' $Y(l)$ with the same wave vector $\boldsymbol{k}$. It will be then convenient to write $M_n^0(a; l_1, l_2, \ldots, l_n; \xi)$ with $a = j$ ($a = \boldsymbol{k}$) to indicate the common site j (wave vector $\boldsymbol{k}$) of all the $l_1, l_2, \ldots, l_n$. It is also convenient to write $M_n(a; l_1, l_2, \ldots, l_n; \xi)$ and $S_m(a; l_1, l_2, \ldots, l_m; \xi)$, and a few of the diagrams that constitute M_2 and S_2 are shown in figures 2(c) and 2(d).

The renormalized M_n in the presence of ξ is now expressed by the relation

$$M_n(a; l_1, \ldots, l_n; \xi) = \left\{ \exp\left[\sum_{r=1}^{\infty} \int \mathrm{d}l_{n+1} \cdots \int \mathrm{d}l_{n+r}\ S_r(a; l_{n+1}, \ldots, l_{n+r}; \xi) \right.\right.$$
$$\left.\left. \times\ \delta_{n+1} \cdots \delta_{n+r} \right] M_n^0(a; l_1, \ldots, l_n; \xi) \right\} \tag{3.1}$$

where

$$\int \mathrm{d}l_s = \sum_{\alpha_s} \sum_{u_s} \int_0^\beta \mathrm{d}\tau_s$$

(changing α_s into σ_s for the conduction vertices).

At the end of the calculation the value $\xi = 0$ is taken, and all of the diagrams that would not contribute are discarded. As Wick's theorem is valid for the C-operators when $\xi = 0$, all the cumulants of c electrons with more than two C-operators can be neglected, but all the cumulants with only one C-operator must be kept throughout the procedure, because application of a single δ_a would transform any of those cumulants into one with two $Y(l)$, which might not vanish when $\xi = 0$ (namely, when the two $Y(l)$ are C-operators with the same $\boldsymbol{k}$, σ and opposite u).

To calculate the self-fields it is also possible to consider only skeleton diagrams without insertions and replace all of the M_n^0 by the renormalized M_n: this would give the renormalized form of the self-field, which can be denoted by $S_m(a; l_1, l_2, \ldots, l_m; M; \xi)$ to emphasize its functional dependence on M. The equation (3.1) becomes then a non-linear equation in M, and its solution would allow the calculation of the GF employing only skeleton diagrams.

The procedure discussed above is equivalent to the calculation with unrenormalized vertices [4], and its validity depends on the fact that all of the diagrams in the calculation are 'rooted' [4], i.e., they have external (fixed) vertices. In the calculation of the free energy, only vacuum diagrams appear, and there is no unique way to associate a skeleton with a given diagram. As the vacuum diagrams have no external vertices, one says that such a diagram is irreducible (the equivalent of a skeleton diagram) when no vertex can be considered to have two or more insertions (any vertex of a vacuum diagram can always be considered to have at least one insertion). The functional $\Phi[M, \xi]$ is then defined as the sum of the contributions of all irreducible and connected vacuum diagrams, when at each vertex the unrenormalized M_n^0 is substituted for with the renormalized M_n. From the definition of $\Phi[M, \xi]$ and the rules for diagram calculation in I, it is clear that the self-fields satisfy the relation (cf. equation (42) in [5])

$$S_m(a; l_1, l_2, \ldots, l_m; M; \xi) = \frac{\delta \Phi[M, \xi]}{\delta\ M_m(a; l_1, l_2, \ldots, l_m; \xi)}. \tag{3.2}$$

Because of overcounting of unrenormalized diagrams, the grand canonical potential (cf. equation (3.19) in I) is not given by $\Omega(\beta, \xi) = \Omega_0(\beta, \xi) - T\Phi[M, \xi]$. To solve this difficulty one writes†

$$\mathcal{Z}_0(\beta, \xi) = \prod_j \mathcal{Z}_0(\beta, j, \xi_j) \prod_{\boldsymbol{k}} \mathcal{Z}_0(\beta, \boldsymbol{k}, \xi_{\boldsymbol{k}}) \tag{3.3}$$

and defines

$$M_0^0(a; \xi) = \ln \mathcal{Z}_0(\beta, a; \xi_a). \tag{3.4}$$

If in equation (2.6) $\ln \mathcal{Z}_0(\beta, \xi)$ is substituted for with $\ln \mathcal{Z}_0(\beta, a; \xi_a)$, the same M_n^0 as defined before are obtained for $n > 0$, while $M_0^0(a; \xi)$ is obtained for $n = 0$. A renormalized $M_0(a; \xi)$ is then defined by equation (3.1) when $M_0^0(a; \xi)$ takes the place of M_n^0 in the right-hand side, and it is equal to $M_0^0(a; \xi)$ plus the sum of the diagrams obtained by making all of the possible insertions at the single vertex a. The overcounting of diagrams in $\Phi[M, \xi]$ can be now corrected by following the derivation due to Bloch and Langer (see [12, 13]) for the Ising model. Because of its topological character, it can be applied directly to our problem by only making the appropriate changes in the calculation of the diagrams.

† In the absence of hybridization one can write the Hamiltonian (with external fields included) as the sum of operators, each one of them containing only $Y(l)$-operators with a single value of j or of $\boldsymbol{k}$. Equation (3.3) holds because all of those operators commute, and the definition of $\mathcal{Z}_0(\beta, a, \xi_a)$ is obvious.

One then obtains

$$\ln \mathcal{Z}(\beta,\xi) = \Phi[M,\xi] + \sum_a M_0(a;\xi) - \sum_{a,n} \int \mathrm{d}l_1 \cdots \int \mathrm{d}l_n \; S_n(a;l_1,\ldots,l_n;\xi) M_n(a;l_1,\ldots,l_n;\xi). \tag{3.5}$$

Note that from the discussion above it follows that all of the diagrams of $\ln \mathcal{Z}_0(\beta,\xi)$ are already included in the right-hand side of equation (3.5) through the $M_0(a;\xi)$.

The cumulant GF are now given by (cf. equations (A.26), (A.28) of I)

$$G_n(l_1,l_2,\ldots,l_n;\xi) = \delta_1\delta_2\cdots\delta_n \ln[\mathcal{Z}(\beta,\xi)] \tag{3.6}$$

and one can prove that

$$G_1(l_1;\xi) = M_1(j;l_1;\xi) \tag{3.7}$$

(cf. equation (85) in [4] for the equivalent property in the Ising model). Although this GF vanishes when $\xi = 0$, equation (3.6) gives

$$G_2(l_1,l_2;\xi) = \frac{\delta M_1(j;l_1;\xi)}{\delta\xi(l_2)} \tag{3.8}$$

which does not necessarily vanish when $\xi = 0$.

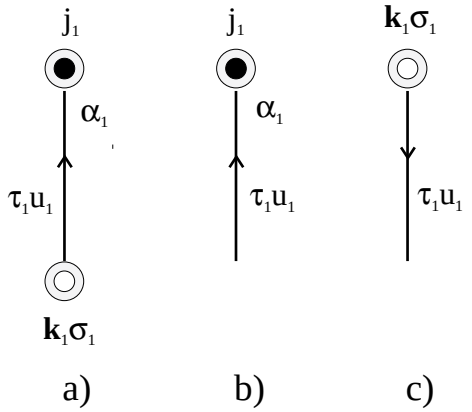

Figure 3. The Φ-derivable approximation that gives the CHA. (a) The skeleton diagram that gives $\bar{\Phi}$. (b) The self-field $\bar{S}_1[\boldsymbol{k}_1,\bar{1},\xi]$, given in equation (A3). (c) The self-field $\bar{S}_1[j_1,1,\xi]$, given in equation (A2).

The relations derived above correspond to the expansion that sums all the diagrams and would give the exact results. The basic philosophy of the Φ-derivable approximation is to select subfamilies of diagrams that give approximate $\bar{\mathcal{Z}}(\beta,\xi)$ by employing equation (3.5), and then generate all the approximate GF by starting from this unique quantity (cf. equation (3.6)). This procedure is expected to give consistent approximations for the different physical quantities involved [4]. The Φ-derivable approximation can then be stated as follows.

Rule 4.1

(a) Choose an approximate $\bar{\Phi}[\bar{M},\xi]$ consisting of a subset of the irreducible diagrams that give the exact $\Phi[M,\xi]$. The approximate $\bar{\mathcal{Z}}(\beta,\xi)$ is obtained from equation (3.5) by employing the approximate $\bar{\Phi}$, $\bar{M}_n$ and $\bar{S}_n$ instead of the exact ones.

(b) Define $\bar{S}_n$ with equation (3.2), employing the approximate $\bar{\Phi}$ and $\bar{M}_n$.

(c) Define $\bar{M}_n$ with equation (3.1), employing the self-fields $\bar{S}_m(a; l_1, l_2, \ldots, l_m; M; \xi)$ defined in (b).

Note that to apply part (b), only $\bar{S}_n$ as a function of the $\bar{M}_n$ is needed, so the relation obtained in part (c) can be considered again as a non-linear equation in the $\bar{M}_n$.

Rule 4.1 is now applied to the simplest possible family of skeleton diagrams with $\xi \neq 0$, which is shown in figure 3(a). Although its contribution vanishes when $\xi = 0$, it nevertheless generates the CHA (cf. figure 1(b)) for the one-particle GF. Φ for this family is

$$\bar{\Phi} = \sum_{j_1,\alpha_1,u_1,k_1,\sigma_1} \int_0^\beta \mathrm{d}\tau_1 \; \bar{M}_1(\boldsymbol{k}_1; \sigma_1, -u_1, \tau_1; \xi) v(j_1, \alpha_1, \boldsymbol{k}_1, \sigma_1, u_1) \bar{M}_1(j_1; \alpha_1, u_1, \tau_1; \xi) \tag{3.9}$$

where $v(j_1, \alpha_1, \boldsymbol{k}_1, \sigma_1, u_1)$ is the hybridization constant defined in equation (3.20) of I for the general model.

The calculation of the one-particle GF in this approximation is given in appendix A. Its Fourier transform, in both space and time, is given by

$$G_{f,\sigma}(\boldsymbol{k}, \omega) \equiv G_2^{ff}(\boldsymbol{k}, \sigma, u = -, \omega) = \frac{-(\mathrm{i}\omega - \varepsilon_{\boldsymbol{k}\sigma}) D_\sigma^0}{(\mathrm{i}\omega - \varepsilon_\sigma)(\mathrm{i}\omega - \varepsilon_{\boldsymbol{k}\sigma}) - |V(\boldsymbol{k})|^2 D_\sigma^0} \tag{3.10}$$

for the f electron, where $D_\sigma^0 = \langle X_{00} \rangle + \langle X_{\sigma\sigma} \rangle$. The corresponding GF for the conduction electrons is

$$G_{c,\sigma}(\boldsymbol{k}, \omega) = \frac{-(\mathrm{i}\omega - \varepsilon_\sigma)}{(\mathrm{i}\omega - \varepsilon_\sigma)(\mathrm{i}\omega - \varepsilon_{\boldsymbol{k}\sigma}) - |V(\boldsymbol{k})|^2 D_\sigma^0}. \tag{3.11}$$

These two equations are exactly the GF of the CHA already studied in I and correspond to the family of diagrams shown in figures 1(b) and 1(c). As was discussed in I, the CHA does not satisfy completeness, and it can be concluded that the Φ-derivable approximation does not guarantee this property by itself. The result is rather conclusive, because it was not necessary to add an extra condition to the maximum order of the cumulants employed, and in this sense one can say that this is an 'exact' approximation. The choice of $\Phi[M, \xi]$ itself is sufficient to restrict the self-fields to only the $S_1(\xi)$, and as a consequence of their vanishing when $\xi = 0$, the cumulants in the GF considered above are restricted to second order only.

The only difference between equations (3.10) and (3.11) and the corresponding GF for $U = 0$ is the presence of the D_σ^0, which is then responsible for all the correlation effects in this approximation. When $U \to \infty$, the correlation makes impossible the occupation of an electron with spin σ at a given site j when $\langle X_{j,\bar{\sigma}\bar{\sigma}} \rangle = 1$, and in that case there is no hybridization with the conduction electron at the same site. The effect of the CHA is then to substitute for this local correlation, different at each site, an average one, equal for all sites, and the hybridization constant $|V(\boldsymbol{k})|^2$ is reduced by the same factor $D_\sigma^0 = 1 - \langle X_{\bar{\sigma}\bar{\sigma}} \rangle$ at all sites. One can then think of the CHA as a sort of mean-field approximation. This interpretation is further supported by the fact that the skeleton diagrams of the Φ-derivable approximation that gives the CHA correspond to the molecular-field approximation in the Ising model [4].

In the Ising model, all of the closed rings are usually added [4, 12] to obtain a better $\Phi[M, \xi]$. In this last case, the self-fields S_2 are not zero and cumulants of any even order should then be used. The difficulty of calculating these cumulants in the quantum case (Hubbard model, PAM) makes it necessary to consider only the lowest-order cumulants

(e.g., to fourth order only), and one could then blame the lack of completeness on this further approximation. The discovery that the CHA is also Φ-derivable settles this question.

4. Complete approximations

In the preceding section, the CHA was shown to be an 'exact' Φ-derivable approximation that does not satisfy completeness (cf. equation (1.1)) in the space of the f electrons (although it is automatically satisfied in zeroth order). At the same time, it seemed puzzling that completeness was satisfied in the space of c electrons for all of the families of diagrams that were considered.

In our study of the problem, we happened to find a particular set of diagrams that satisfied completeness in the f space: this led us to formulate the conjecture stated below, which we have verified for many other families of diagrams but could not prove in general. This conjecture also explains why completeness is satisfied in c space by any family of diagrams.

Conjecture

Completeness is satisfied when the family of diagrams obeying theorem 3.3 in I, which is employed to approximate the one-particle GF, is such that:

(1) for any open diagram with external vertices i and j, there is also a closed diagram obtained by 'joining' i and j into a single vertex j; and

(2) for any diagram with only one external vertex at a site j, there are also all of the possible open diagrams obtained by 'separating' j into a pair of different vertices i and j.

Any family of GF diagrams that satisfies this conjecture will be called a 'complete-cumulant approximation' (CCA) in what follows. It should be emphasized that we have verified this conjecture only with families of diagrams that have cumulants of a maximum order of four; some of them have diagrams with an infinite number of fourth-order cumulants, but they will not be discussed here.

The conjecture above implies that any family of diagrams for the c-electron GF should be complete, because joining two external vertices i and j of a diagram would give a single vertex joined by at least four edges; by Wick's theorem, the corresponding cumulant vanishes, and so does the contribution of the diagram.

In general, the CCA are not Φ-derivable, because their corresponding family of diagrams would not have all those that result by dressing the f vertices of a family of skeleton diagrams. The simplest Φ-derivable approximation is the CHA, derived from the skeleton diagram in figure 3(a), and to make it a CCA it is necessary to add all of the diagrams shown in figure 4(b), as will be discussed in the following section, 4.1. These last diagrams correspond to adding a particular set of decorations to the first diagram of figure 4(a) but not to all the infinite diagrams represented by the second diagram of the same figure, so it is clear that this CCA is not Φ-derivable. In general, any 'exact' Φ-derivable approximation containing simple loops as self-fields would have diagrams with unrenormalized cumulants of any even order, and this would not be the case for most CCA.

The simplest possible family of diagrams that give a CCA is illustrated in figure 1(a), and the corresponding GF verify the conjecture above, both in the atomic limit [14, 15] and for a rectangular band.

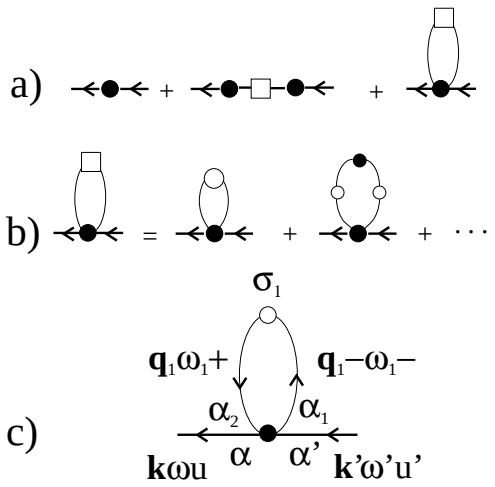

Figure 4. (a) The complete-chain approximation: empty squares symbolize the diagrams of the c-electron GF in the CHA (cf. figure 1(c)). (b) The diagrams added to the CHA to make it complete. (c) The simplest diagram in (b) with the indices employed in the calculation of appendix A.

4.1. The complete-chain approximation

To calculate the occupation numbers at a site j, the GF at that site $G_{f;\sigma}(j,\omega)$ are needed. The corresponding diagrams for the CHA are shown in figure 1(b), and following our conjecture a CCA is obtained by adding all of the diagrams obtained by joining in that figure the external vertices i and j of the chains of any length. This approximation will be called a 'complete-chain approximation' (c-CHA) and its family of diagrams is shown in figure 4(a). The corresponding GF will be denoted by $G^{C}_{f;\sigma}(\omega)$, where the site index j was dropped because of the invariance under lattice translations. It has two contributions:

$$G^{C}_{f;\sigma}(\omega) = C_{f,\sigma}(\omega) + S^{CH}_{\sigma}(\omega) \tag{4.1}$$

where $C_{f,\sigma}(\omega)$ is the GF at site j obtained for the CHA (cf. equation (4.2) below, which employs equation (3.10)) and $S^{CH}_{\sigma}(\omega)$ is the contribution of the diagrams with loops, added to the CHA to make it a CCA (cf. figure 4(b)).

As in I, a local hybridization interaction $V(\boldsymbol{k},\sigma) = V$ will be considered, as well as a rectangular band of width $2W$ for the unperturbed conduction electrons, centred at the energy E_0. The corresponding density of states per unit energy, per site and per spin component is then $\rho_0(\omega) = \rho_0 = 1/(2W)$ for $-W + E_0 < \omega + \mu < W + E_0$. Here ω is a real energy variable, and it is shifted by μ because the averages are taken in the grand canonical ensemble. The contribution of the first term is given by

$$C_{f,\sigma}(\omega) \equiv \frac{1}{N}\sum_{\boldsymbol{k}} G_{f,\sigma}(\boldsymbol{k},\omega) = G^{0}_{f,\sigma}(\omega)\left\{1 - G^{0}_{f,\sigma}(\omega)\rho_0|V|^2 \ln\left[R^{0}(\omega)\right]\right\} \tag{4.2}$$

where

$$R^{0}(\omega) = (\mathrm{i}\omega - \varepsilon^{m}_{1})(\mathrm{i}\omega - \varepsilon^{m}_{2})/((\mathrm{i}\omega - \varepsilon^{M}_{1})(\mathrm{i}\omega - \varepsilon^{M}_{2}))$$

and

$$G^{0}_{f,\alpha,u}(\omega) = -D^{0}_{\alpha}/(\mathrm{i}\omega - u\varepsilon_{\alpha}).$$

The ε_i^m and ε_i^M are respectively the minimum and maximum values of each of the two 'bands' $\varepsilon_{i,\sigma}(\boldsymbol{k})$ in the CHA, where $i = 1$ corresponds to the 'upper band' and $i = 2$ to the 'lower band':

$$\varepsilon_{i,\sigma}(\boldsymbol{k}) = \frac{1}{2}\left\{\varepsilon_{\boldsymbol{k}\sigma} + \varepsilon_{f\sigma} \pm \sqrt{(\varepsilon_{\boldsymbol{k}\sigma} - \varepsilon_{f\sigma})^2 + 4D_\sigma^0|V_{\boldsymbol{k}}|^2}\right\}. \tag{4.3}$$

The corresponding quantity for the c electrons

$$C_{c,\sigma}(\omega) \equiv \frac{1}{N}\sum_{\boldsymbol{k}} G_{c,\sigma}(\boldsymbol{k},\omega) = \rho_0 \ln\left[R^0(\omega)\right] \tag{4.4}$$

appears in the calculation of $S_\sigma^{CH}(\boldsymbol{k},\omega)$ (cf. figure 4), which also requires cumulants with four X-operators of the 'Fermi type'. As discussed before, all of the cumulants of order higher than two vanish when the corresponding operators satisfy Wick's theorem, and one can then use standard diagrammatic expansions. The higher-order cumulants of X-operators are non-zero because of the correlations that are built into the ionic states by the infinite Coulomb repulsion and are hidden into the 'free-ion' Hamiltonian $\mathcal{H}_0$ of equation (2.4). The calculation of the necessary X-cumulants is discussed in appendix B and that of $S_\sigma^{CH}(\omega)$ is summarized in appendix C. In the reciprocal space, $S_\sigma^{CH}(\boldsymbol{k},\omega)$ does not depend on $\boldsymbol{k}$, so $S_\sigma^{CH}(\omega) = S_\sigma^{CH}(\boldsymbol{k},\omega)$, and the following expression was obtained:

$$S_\sigma^{CH}(\omega) = \frac{1}{N}\sum_{\boldsymbol{k}} S_\sigma^{CH}(\boldsymbol{k},\omega) = -|V|^2(AK_\sigma(\omega) + BK_\sigma^2(\omega)C_{c,\sigma}(\omega) + CK_\sigma^2(\omega)) \tag{4.5}$$

where $A = [D_\sigma^0(1 - D_\sigma^0) - x_\sigma^2]\beta I_1 - D_\sigma^0 I_2$; $B = -D_\sigma^0(1 - D_\sigma^0) + x_\sigma$; and $C = -D_\sigma^0 I_1$; $x_\sigma = \langle X_{\sigma\sigma}\rangle$; and

$$I_\ell = \frac{1}{\beta}\sum_{\omega_1} C_{c,\sigma}(\omega_1)K_\sigma^\ell(\omega_1) \qquad \text{(with } \ell = 1, 2\text{)}. \tag{4.6}$$

$C_{c,\sigma}(\omega)$ is given by equation (4.4), and $K_\sigma(\omega_s) = -1/(\mathrm{i}\omega_s - \varepsilon_{f\sigma}) = G_{f,\sigma}^0(\omega_s)/D_\sigma^0$. The GF of c electrons in the c-CHA are the same as in the CHA, because the cumulants of order greater than two vanish for the C-operators $Y(l)$.

The analytic continuation $\bar{G}_{f;\sigma}^C(z)$ of equation (4.1) has singularities on the real axis only: they are two branch cuts on the intervals $[\varepsilon_j^m,\varepsilon_j^M]$ (with $j = 1, 2$) as well as first- and second-order poles at $\varepsilon_{f\sigma}$. The integral of the spectral density $\rho_f(\omega)$ of equation (2.11) along the real axis gives the modified $D_\sigma = \langle X_{00}\rangle_{\mathcal{H}} + \langle X_{\sigma\sigma}\rangle_{\mathcal{H}}$, but in the present case it is better to perform the ω-integration before the sum over $\boldsymbol{k}$. The ω-integration can then be replaced by a complex integration of the analytic continuations $\bar{G}_{f,\sigma}(\boldsymbol{k},z) + \bar{S}_\sigma^{CH}(\boldsymbol{k},z)$ along a contour surrounding the real axis, and it is not difficult to show that only the first-order poles at $\varepsilon_{f\sigma}$ of these two functions contribute, giving the $\boldsymbol{k}$-independent value $D_\sigma^0 - A|V|^2$. The subsequent sum over all of the $\boldsymbol{k}$-states gives then the same result for any unperturbed density of states $\rho_c^0(\varepsilon_{\boldsymbol{k}})$ of the c electrons. The f-electron occupation number is given by equation (2.10) and can be calculated in a similar way, but all of the terms of $\bar{G}_{f;\sigma}^C(z)$ contribute because of the presence of the Fermi function in the integrand. The result depends on the unperturbed energy $\varepsilon_{\boldsymbol{k}}$ of the c electrons, and we could not find a general analytical result for arbitrary $\rho_c^0(\varepsilon_{\boldsymbol{k}})$, so the integration over $\varepsilon_{\boldsymbol{k}}$ (i.e. the sum over $\boldsymbol{k}$) had to be performed numerically for each density of states.

The values of the occupation number per site and per spin of the f electrons $n_{f,j,\sigma} = \langle X_{j,\sigma\sigma}\rangle_{\mathcal{H}}$ and of the c electrons $n_{c,j,\sigma} = \langle C_{j,\sigma}^\dagger C_{j,\sigma}\rangle_{\mathcal{H}}$ were calculated for representative values of the model's parameters within the c-CHA. The averages at different sites and for the two values of σ are equal when the system is paramagnetic and invariant under lattice

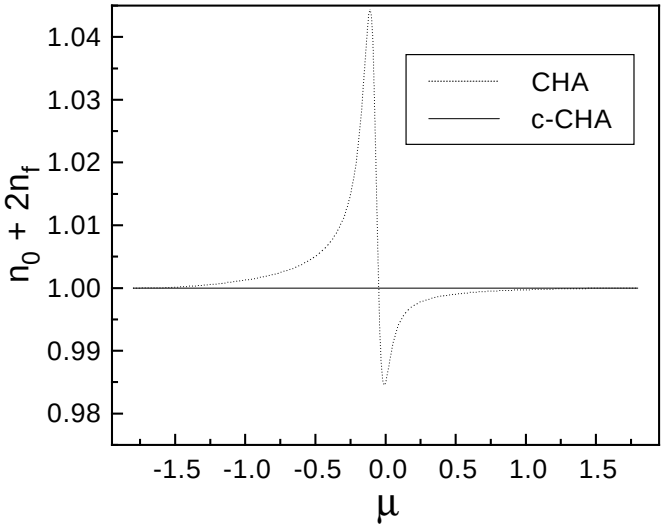

Figure 5. The quantity $2n_f + n_0$ is plotted as function of the chemical potential μ to test completeness for the CHA and the c-CHA in the atomic limit, i.e., for a conduction band of zero width. The following set of parameters was employed: $E_f = -0.05$, $V = 0.1$ and $T = 0.025$, all measured in the same energy units.

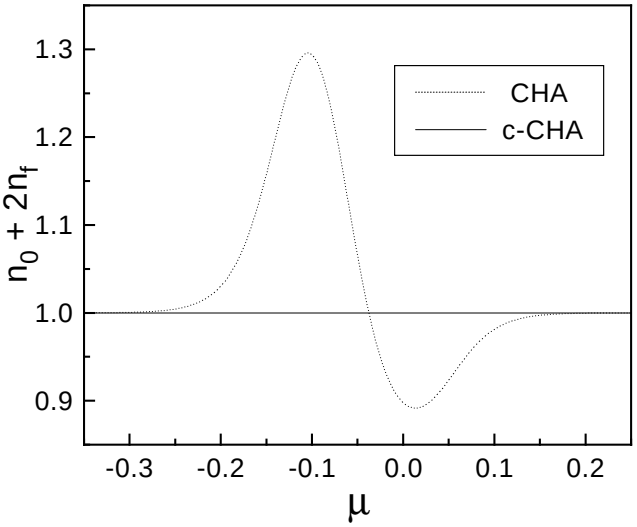

Figure 6. The same type of plot as in figure 5, but for a rectangular band of width $2W = \pi$, with the same parameters as employed in that figure.

translations, and one can then write $n_f = n_{f,j,\sigma}$ and $n_c = n_{c,j,\sigma}$. The quantity $2n_f + n_0$ is plotted in figure 5 against the chemical potential μ for both the CHA and the c-CHA in the atomic limit [15] for $E_{j\sigma} = E_f = -0.05$, $V = 0.1$ and $T = 0.025$, all measured in the same energy units. The same values are employed in figure 6 for a rectangular band of width $2W = \pi$. In these figures it is clear that the c-CHA satisfy completeness while the CHA does not.

One interesting question is whether the completeness obtained with our conjecture is an artifact of the particular choice of a rectangular density of states $\rho_c^0(\varepsilon_{\boldsymbol{k}})$ and of the local hybridization. In the case of the c-CHA, it was not difficult to repeat the numerical calculations for other densities of states and also for nearest-neighbour hybridization. All of the combinations of either local or nearest-neighbour hybridization with the $\rho_c^0(\varepsilon_{\boldsymbol{k}})$ of a chain with nearest-neighbour hopping and also of a Gaussian density of states were employed, and in all cases completeness was obtained for the c-CHA.

5. Summary and conclusions

We have studied the Φ-derivable approximation, which had already been applied to the Ising model [4, 12, 13], and was shown by Kadanoff and Baym [9] to have important conservation properties. We have been able to find the skeleton diagram (cf. figure 3(a)) that gives the CHA: its contribution vanishes when $\xi = 0$, but generates all of the diagrams of the CHA that remain in that limit. This skeleton gives an 'exact' Φ-derivable approximation, because only second-order cumulants appear when $\xi = 0$, and it is therefore not necessary to neglect contributions of higher-order cumulants which are too laborious to calculate. As was shown in I, the CHA approximation does not satisfy completeness, and it then follows that the use of a Φ-derivable approximation would not guarantee that property.

Although this result settled one problem, it was still necessary to find a systematic way of choosing families of diagrams that would satisfy completeness. Analysing different families, one was found with the desired property. This led us to advance the conjecture stated in section 4, which was tested with several families of diagrams that have infinite cumulants of at most fourth order, although it was not verified for diagrams with higher-order cumulants. Increasing the family of diagrams of the CHA with those required to satisfy the conjecture defines a new approximation, which was called the c-CHA. Completeness was tested numerically for the c-CHA, and the results presented in section 4 are excellent. As discussed in section 4, another result that follows from the conjecture is the proof that all of the families of diagrams for the c-electron GF are complete.

It should be noticed that the GF derived with the CHA is formally similar to those found in Gutzwiller's treatment [16] of the PAM and in the lowest approximation of the slave-boson formulation [17]. In those two methods, two hybridized bands of uncorrelated electrons are obtained, but with a renormalized energy $\widetilde{\epsilon}_f$ of the local electron. Completeness is automatically satisfied in those bands, and the effect of correlations is achieved by forcing $n_f < 0.5$ through an adequate choice of $\widetilde{\epsilon}_f$, which should then be rather close to the Fermi energy. Differently from these two methods, the correlations are automatically built up in the Hubbard operators employed in the present calculation. In the CHA, as in other methods [7], an energy renormalization is not found [18]. We believe that the renormalization would be obtained in the cumulant expansion by adding extra diagrams to the CHA and making further approximations to the expressions obtained.

5.1. Conclusions

The results presented here appear to advance the understanding of the diagrammatic cumulant expansion in the following respects.

(1) A conjecture that shows how to choose families of GF diagrams that would satisfy completeness is proposed and verified, employing different types of densities of states of the c electrons, as well as local and nearest-neighbour hybridization in a simple cubic lattice.

(2) It is shown that the CHA is an 'exact' Φ-derivable approximation that does not satisfy completeness.

(3) The GF of the CHA and of the c-CHA are analytical off the real axis. The behaviour of the spectral density is rather good, but important features like the Kondo resonance are absent in the spectral densities of the CHA and of the c-CHA, although the last one contains diagrams which have one cumulant with spin-flip processes.

(4) A deeper understanding of why the conjecture is true, at least for the diagrams with fourth-order cumulants at most, is still lacking.

Acknowledgments

The authors would like to thank Professor Roberto Luzzi for critical comments, and to acknowledge financial support from the following agencies: CAPES-PICD (MSF), FAPESP, CNPq, and FAEP-UNICAMP (MEF).

Appendix A. Calculation of the GF for the CHA as a Φ-derivable approximation

In this appendix, the details of the derivation of the GF for the CHA as a Φ-derivable approximation are given. The $\bar{\Phi}$ of equation (3.9) is given here in abbreviated notation:

$$\bar{\Phi} = \sum_{j_1,\alpha_1,u_1,k_1,\sigma_1} \int_0^\beta \mathrm{d}\tau_1 \; \bar{M}_1(\boldsymbol{k}_1;\bar{1};\xi) v(j_1,\boldsymbol{k}_1,1)\bar{M}_1(j_1;1;\xi) \tag{A1}$$

where $M_1(j_1;\alpha_1,u_1,\tau_1;\xi) = M_1(j_1;1;\xi)$ and $M_1(\boldsymbol{k}_1;\sigma_1,-u_1,\tau_1;\xi) = M_1(\boldsymbol{k}_1;\bar{1};\xi)$. It is also convenient to use the slightly different notation $v(j_1,\alpha_1,\boldsymbol{k}_1,\sigma_1,u_1) = v(j_1,\boldsymbol{k}_1,1)$ and $v(j_1,\alpha_1,\boldsymbol{k}_1,\sigma_1,-u_1) = v(j_1,\boldsymbol{k}k_1,\bar{1})$ for the hybridization constant (here the abbreviation (1) includes α_1,σ_1,u_1 but it does not include τ_1).

Equation (3.2) is now employed to obtain the corresponding self-fields:

$$\bar{S}_1(j_1;1;\xi) = \sum_{\boldsymbol{k}_1\sigma_1} v(j_1,\boldsymbol{k}_1,1)\bar{M}_1(\boldsymbol{k}_1;\bar{1};\xi) \tag{A2}$$

and

$$\bar{S}_1(\boldsymbol{k}_1;\bar{1};\xi) = \sum_{j_1\alpha_1} v(j_1,\boldsymbol{k}_1,1)\bar{M}_1(j_1;1;\xi). \tag{A3}$$

All of the remaining self-fields S_n with $n \geqslant 2$ reduce to zero in this approximation, and equation (3.1) gives the renormalized $\bar{M}_1(a;\xi)$, namely

$$\bar{M}_1(j;1;\xi) = \exp\left\{\int \mathrm{d}2 \; \bar{S}_1(j;2;\xi)\frac{\delta}{\delta\xi(j;2)}\right\} M_1^0(j;1;\xi) \tag{A4}$$

and

$$\bar{M}_1(\boldsymbol{k};1;\xi) = \exp\left\{\int \mathrm{d}2 \; \bar{S}_1(\boldsymbol{k};2;\xi)\frac{\delta}{\delta\xi(\boldsymbol{k};2)}\right\} M_1^0(\boldsymbol{k};1;\xi). \tag{A5}$$

The GF

$$\begin{aligned} G_{j,j',2}(1,1';\xi) &= \frac{\delta\bar{M}_1(j;1;\xi)}{\delta\xi(j',1')} \\ &= \bar{M}_2(j;1;1';\xi)\delta(j,j') + \int \mathrm{d}2 \; \bar{M}_2(j;1;2;\xi)\frac{\delta\bar{S}_1(j;2;\xi)}{\delta\xi(j',1')} \end{aligned} \tag{A6}$$

is obtained from equation (3.8), and from equation (A2) it follows that

$$G_{j,j',2}(1;1';\xi) = \bar{M}_2(j;1;1';\xi)\delta(j,j') + \sum_{\boldsymbol{k}_2}\int \mathrm{d}2\ \bar{M}_2(j;1;2;\xi)v(j,\boldsymbol{k}_2,2)G_{\boldsymbol{k}_2,j',2}(\bar{2},1';\xi). \tag{A7}$$

A mixed GF appears in the right-hand side of this last equation, and from equations (3.8) and (A5) it is given by

$$G_{\boldsymbol{k},j',2}(\bar{1};1';\xi) = \frac{\delta\bar{M}_1(\boldsymbol{k};\bar{1};\xi)}{\delta\xi(j',1')} = \frac{\delta}{\delta\xi(j',1')}\exp\left\{\int \mathrm{d}2\ \bar{S}_1(\boldsymbol{k};2;\xi)\frac{\delta}{\delta\xi(\boldsymbol{k};2)}\right\}M_1^0(\boldsymbol{k};\bar{1},\xi). \tag{A8}$$

Calculaing the derivatives, and observing that when $\xi = 0$ the conduction cumulants of order greater than two vanish, it follows that

$$G_{\boldsymbol{k},j',2}(\bar{1};1';\xi) = \int \mathrm{d}2\ \frac{\delta\bar{S}_1(\boldsymbol{k};2;\xi)}{\delta\xi(j',1')}\bar{M}_2(\boldsymbol{k};\bar{1};2;\xi). \tag{A9}$$

The derivatives of the self-fields S_1 can be calculated from equation (A3) and then replaced in equation (A9). Substituting this result in equation (A7), the required GF is obtained:

$$G_{j,j',2}(1;1';\xi) = \bar{M}_2(j;1;1';\xi)\delta(j,j') + \sum_{\boldsymbol{k}_2,j_3}\int \mathrm{d}2\ \mathrm{d}3\ \bar{M}_2(j;1;2;\xi) \times v(j,\boldsymbol{k}_2,2)v(j_3,\boldsymbol{k}_2,\bar{3})\bar{M}_2(\boldsymbol{k}_2;\bar{2},3;\xi)G_{j,j_3,2}(\bar{3};1',\xi). \tag{A10}$$

The Grassmann fields ξ are 'turned off' to recover the invariance under lattice translations, and the ionic cumulants then become site independent. The site indices are not necessary any more, and will not be explicitly indicated in the following. The spatial Fourier transform of equation (A10) then gives

$$G_2^{ff}(\boldsymbol{k},\alpha,u,\tau;\boldsymbol{k}',\alpha',u',\tau') = \Delta(u\boldsymbol{k}+u'\boldsymbol{k}')\,\Delta(u+u')\,\bar{M}_2(f;\alpha,u,\tau,\alpha',u,\tau')) + \sum_{\alpha_1\sigma_1}\sum_{\alpha_2\sigma_2}\int_0^\beta \mathrm{d}\tau_1\ \mathrm{d}\tau_2\ \bar{M}_2(f;\alpha,u,\tau;\alpha_1,u',\tau_1)\bar{M}_2(\boldsymbol{k};\sigma_1,u,\tau_1,\sigma_2,u',\tau') \times V(\alpha_1,\boldsymbol{k},\sigma_1,u')V(\alpha_2,\boldsymbol{k},\sigma_2,u)G_2^{ff}(\boldsymbol{k},\alpha_2,u,\tau_2,\boldsymbol{k}',\alpha',u',\tau') \tag{A11}$$

where all the indices are indicated explicitly. All of the GF are now functions of the wave vectors $\boldsymbol{k}$, and the notation G_2^{ff} and G_2^{cc} is used to distinguish between them. The summation over the dummy u-indices has been already performed in equation (A11), and $\Delta(\boldsymbol{k}) = \delta(\boldsymbol{k},0)$.

The time Fourier transform of equation (A11) then gives

$$G_2^{ff}(\boldsymbol{k},\alpha,u,\omega;\boldsymbol{k}',\alpha',u',\omega') = \Delta(u\boldsymbol{k}+u'\boldsymbol{k}')\Delta(u+u')\Delta(\omega+\omega')\bar{M}_2(f;\alpha,u,\omega,\alpha',u',\omega') + \sum_{\alpha_1\sigma_1}\sum_{\alpha_2\sigma_2}\bar{M}_2(f;\alpha,u,\omega;\alpha_1,u',-\omega)\bar{M}_2(\boldsymbol{k};\sigma_1,u,-\omega;\sigma_2,u',\omega) \times V(\alpha_1,\boldsymbol{k},\sigma_1,u')V(\alpha_2,\boldsymbol{k},\sigma_2,u)G_2^{ff}(\boldsymbol{k},\alpha_2,u,\omega,\boldsymbol{k}',\alpha',u',\omega') \tag{A12}$$

where (cf. equation (3.38) in I)

$$v(j,\alpha,\boldsymbol{k},\sigma,u) = V(\alpha,\boldsymbol{k},\sigma,u)N_s^{-1/2}\exp(\mathrm{i}u\boldsymbol{k}\cdot\boldsymbol{R}_j). \tag{A13}$$

The inhomogeneous term of equation (A12) vanishes unless $\omega' = -\omega$, $u' = -u$ and $\boldsymbol{k}' = -\boldsymbol{k}$, and when the Hamiltonian is independent of spin, this last equation is easily solved for the PAM with $U = \infty$. Writing σ in place of $\alpha = (0\sigma)$ the solution is given by

$$G_2^{ff}(\boldsymbol{k}, \sigma, u, \omega) = \frac{\bar{M}_2(f; \sigma, u, \omega)}{1 - |V(\boldsymbol{k}, \sigma)|^2 \bar{M}_2(\boldsymbol{k}; \sigma, u, \omega)\bar{M}_2(f; \sigma, u, \omega)} \tag{A14}$$

where the following abbreviations were employed:

$$G_2^{ff}(\boldsymbol{k}, \sigma, u, \omega) \equiv G_2^{ff}(\boldsymbol{k}, \sigma, u, \omega; -\boldsymbol{k}; \sigma, -u, -\omega)$$
$$\bar{M}_2(f; \sigma, u, \omega) \equiv \bar{M}_2(f; \sigma, u, \omega; \sigma, -u, -\omega)$$
$$\bar{M}_2(\boldsymbol{k}; \sigma, u, \omega) \equiv \bar{M}_2(\boldsymbol{k}; \sigma, u, -\omega; \sigma, -u, \omega)$$
$$|V(\boldsymbol{k}, \sigma)|^2 = V(0\sigma, \boldsymbol{k}, \sigma, -u)V(0\sigma, \boldsymbol{k}, \sigma, u).$$

The self-fields $\bar{S}_1$ vanish for $\xi = 0$, and the renormalized $\bar{M}_2$ coincide then with the M_2^0 (cf. equation (3.1)), so

$$\bar{M}_2(f; \sigma, u, \omega) = M_2^0(f; \sigma, u, \omega) = -\frac{D_\sigma^0}{\mathrm{i}\omega + u\epsilon_\sigma} \tag{A15}$$

and

$$\bar{M}_2(\boldsymbol{k}; \sigma, u, \omega) = M_2^0(\boldsymbol{k}; \sigma, u, \omega) = -\frac{1}{\mathrm{i}\omega + u\epsilon_{k\sigma}} \tag{A16}$$

where the unrenormalized cumulants are equal to the free one-electron GF of the f electrons and c electrons respectively, and can be obtained from the rules in I [14, 19]. Substituting these relations in equation (A14), one obtains the localized GF of the CHA, already given in equations (3.10) and (3.11).

Appendix B. The generalized version of Wick's theorem

When resorting to the diagrammatic expansion of I it is necessary to calculate cumulants of X-operators at each local vertex of the diagram (cf. rule 3.5 in I). As physical properties are obtained in the absence of the Grassmann fields ξ (one has to set $\xi = 0$ at the end of the calculation), only $\xi = 0$ will be considered here. The cumulants required in the expansion are $\langle (Y(\gamma_1, \tau_1) \cdots Y(\gamma_n, \tau_n))_+ \rangle_c$ (where all the $\gamma_i = (f; j_s, \alpha_i, u_i)$ correspond to the same site j_s). To calculate them it is sufficient to know [10] the usual averages $\langle (Y(\gamma_1, \tau_1) \cdots Y(\gamma_r, \tau_r))_+ \rangle$ which can be obtained from all the partitions of the $Y(\gamma_i, \tau_i)$ that appear in the cumulant, and the cumulants are then obtained by inverting relations like equation (3.16) in I. The averages required have all the $Y(\gamma_i, \tau_i)$ at the same site, and are given by

$$\langle (Y(\gamma_1, \tau_1) \cdots Y(\gamma_n, \tau_n))_+ \rangle = \frac{\mathrm{Tr}\{\exp(-\beta\mathcal{H}_0)(Y(\gamma_1, \tau_1) \cdots Y(\gamma_n, \tau_n))_+\}}{\mathrm{Tr}\{\exp(-\beta\mathcal{H}_0)\}}. \tag{B1}$$

The usual averages of Fermi or Bose operators are calculated in a systematic way by employing a statistical version of Wick's theorem. A derivation of this theorem [20], based in the commutation or anticommutation relations of the Fermi or Bose operators, was extended [21] to more general operators of the Bose type, and this treatment was further generalized [6] to Fermi-type operators. The technique is based on reducing the average of n operators $Y(\gamma, \tau)$ to a linear combination of averages of $n - 1$ operators $Y(\gamma, \tau)$. This procedure is repeated until averages of only two $Y(\gamma, \tau)$ remain, as is the case with Wick's theorem. The resulting expression is rather more complicated than Wick's theorem

because each commutator or anticommutator of X-operators gives a linear combination of up to two other X-operators rather than a number, as happens with bosons or fermions. It is interesting to note that Wick's theorem is obtained from theorem 3.1 in I when all of the cumulants with more than two operators $Y(\gamma, \tau)$ are zero.

The reduction rule, which expresses the simple averages of n operators $Y(\gamma, \tau)$ as a linear combination of averages with $n-1$ operators $Y(\gamma, \tau)$, will be stated here without derivation, which follows that of Yang and Wang [21]. The only modification is the determination of the correct sign for each term, because the $Y(\gamma, \tau)$ can be Fermi-type operators.

In this appendix all of the $Y(\gamma, \tau)$ correspond to f electrons at the same site, and $\gamma = (b, a)$ serves only to characterize the transitions $|a\rangle \rightarrow |b\rangle$. The restriction that $|b\rangle$ is to have one electron less than $|a\rangle$ will be lifted in this appendix, because more general operators Y_γ appear in the calculation of the averages, and this extension would also allow us to consider a rather arbitrary scheme of levels for $|a\rangle$ and $|b\rangle$, as was done in the general model of section 2 in I.

Employing the general Hamiltonian $\mathcal{H}_f$ of the free f electrons (cf. section 2 in I), it is straightforward to prove

$$\exp(-\beta\mathcal{H}_f) = \sum_c (\exp(-\beta\varepsilon_c))X_{cc} \tag{B2}$$

and from this equation follows the basic relation used to prove the reduction rule:

$$Y(\gamma, \tau)\ \exp(-\beta\mathcal{H}_f) = \exp[\beta\varepsilon(\gamma)] \exp(-\beta\mathcal{H}_f)\, Y(\gamma, \tau) \tag{B3}$$

as well as

$$Y(\gamma, \tau) = Y(\gamma)\ \exp[\beta\varepsilon(\gamma)]. \tag{B4}$$

where $\varepsilon(\gamma) = \varepsilon_b - \varepsilon_a$ corresponds to the transition γ, i.e. to $|a\rangle \rightarrow |b\rangle$.

Before stating the reduction rule it is convenient to define several quantities associated with any pair of operators $Y(\gamma_r)$ and $Y(\gamma_s)$: first,

$$[Y(\gamma_r, \tau_r); Y(\gamma_s, \tau_s)]_\eta = Y(\gamma_r, \tau_r)Y(\gamma_s, \tau_s) - \eta_{rs}Y(\gamma_s, \tau_s)Y(\gamma_r, \tau_r) \tag{B5}$$

where $\eta_{rs} = -1$ if both operators are of the Fermi type, and $\eta_{rs} = +1$ otherwise; and second,

$$\eta(\gamma_r) = \begin{cases} -1 & \text{if } Y(\gamma_r) \text{ is of the Fermi type} \\ +1 & \text{if } Y(\gamma_r) \text{ is of the Bose type.} \end{cases} \tag{B6}$$

The basic relation for the calculation of the usual averages is the *reduction rule*: given the average $\langle (Y(\gamma_1, \tau_1) \cdots Y(\gamma_n, \tau_n))_+ \rangle$ choose one operator $Y(\gamma_i, \tau_i)$ which will be called the 'generator', in such a way that the two states $|a_i\rangle$ and $|b_i\rangle$ in γ_i are not identical; then the following relation holds:

$$\begin{aligned} \langle (Y(\gamma_1, \tau_1) \cdots Y(\gamma_n, \tau_n))_+ \rangle = \sum_{r \neq i} N(i, r) K(\gamma_i, \tau_i - \tau_r) \langle (Y(\gamma_1, \tau_1) \cdots Y(\gamma_{r-1}, \tau_{r-1}) \\ \times [Y(\gamma_r, \tau_r); Y(\gamma_i, \tau_r)]_\eta Y(\gamma_{r+1}, \tau_{r+1}) \cdots Y(\gamma_n, \tau_n))_+ \rangle. \end{aligned} \tag{B7}$$

In this expression:

(i) in each term of the right-hand side, the $Y(\gamma_i, \tau_i)$ from the original average has disappeared, and one $Y(\gamma_r, \tau_r)$ of the original average has been substituted for with $[Y(\gamma_r, \tau_r); Y(\gamma_i, \tau_r)]_\eta$ with $Y(\gamma_i, \tau_r)$ *at the same imaginary time of* $Y(\gamma_r, \tau_r)$;

(ii) $N(i,r)=-1$ if $Y(\gamma_i)$ is of the Fermi type, and there are an odd number of Fermi-type operators that $Y(\gamma_i)$ has to cross *to appear just to the left of* $Y(\gamma_r)$, and $N(i,r)=+1$ otherwise; and

(iii) we have

$$K(\gamma_i,\tau)=\exp[\tau\varepsilon(\gamma_i)]\{(\theta(\tau)+\theta(-\tau)\eta(\gamma_i)\exp[\beta\varepsilon(\gamma_i)])/(1-\eta(\gamma_i)\exp[\beta\varepsilon(\gamma_i)])\}.$$

The restriction that the generator should not be an operator X_{cc} is not important for averages with few operators, because in this case the direct calculation is simple. Nevertheless, we have derived a reduction rule for this type of generator, but it will not be given here because it is not necessary in the present work.

As in this appendix there is no restriction on the two states $|a\rangle$ and $|b\rangle$, the u in $\gamma=(\alpha,u)$ is superfluous, and only the transition α will be given. As the Fourier transform of the cumulants is usually employed (cf. equation (3.32) of I), the transform of the $K(\gamma,\tau)=K(\alpha,\tau)$ given above is necessary, and it is given by $K(\alpha,\omega)=-1/(\mathrm{i}\omega+\varepsilon_\alpha)$.

This $K(\gamma,\omega)$ is valid for the X_α of both Fermi and Bose type, and it has a much simpler structure than $K(\gamma,\tau)$. The corresponding GF is in this case

$$G_\alpha^{(\eta)}(\tau)=\theta(\tau)\langle X_\alpha(\tau)X_\alpha^+\rangle+\eta(\alpha)\theta(-\tau)\langle X_\alpha^+X_\alpha(\tau)\rangle$$

and it is related to the $K(\gamma,\omega)$ by $G_\alpha^{(\eta)}(\omega)=D_\alpha^{(\eta)}K(\gamma,\omega)$ where $D_\alpha^{(\eta)}=\langle X_{bb}\rangle-\eta(\alpha)\langle X_{aa}\rangle$.

The cumulants with four operators that appear in the present work are given by

$$\begin{aligned}\langle(X_\alpha(\omega_1)\bar X_\alpha(\omega_2)X_{\alpha'}(\omega_3)\bar X_{\alpha'}(\omega_4))_+\rangle_c&=\delta_{\alpha\alpha'}D_\alpha(1-D_\alpha)K_\alpha(\omega_1)K_\alpha(\omega_3)\\&\times\{\Delta(\omega_1+\omega_2)\Delta(\omega_3+\omega_4)-\Delta(\omega_3+\omega_2)\Delta(\omega_1+\omega_4)\}\\&-(1-\delta_{\alpha\alpha'})\{\langle X_{\sigma\sigma}\rangle^2_{\mathcal{H}_0}K_\alpha(\omega_1)K_{\alpha'}(\omega_3)\Delta(\omega_1+\omega_2)\Delta(\omega_3+\omega_4)\\&+\langle X_{\sigma\sigma}\rangle_{\mathcal{H}_0}K_\alpha(\omega_3)K_{\alpha'}(\omega_1)\Delta(\omega_3+\omega_2)\Delta(\omega_1+\omega_4)+\beta^{-1}(D_\alpha K_\alpha(\omega_1)\\&+D_{\alpha'}K_{\alpha'}(\omega_3))K_\alpha(-\omega_2)K_{\alpha'}(-\omega_4)\Delta(\omega_1+\omega_2+\omega_3+\omega_4)\}.\end{aligned}\tag{B8}$$

Appendix C. The calculation of $S_\sigma^{CH}(\omega)$

The infinite graphs that contribute to $S_\sigma^{CH}(\boldsymbol{k},\omega)$ are shown in figure 4(b), and the simplest one that is not included in the CHA will be considered first. This graph is repeated in figure 4(c) to identify all the indices necessary to calculate its contribution. From the rule 3.7 and equation (3.33) in I, one obtains in this approximation

$$\begin{aligned}&\langle(\widehat Y(f;\boldsymbol{k},\alpha,u,\omega)\widehat Y(f;\boldsymbol{k}',\alpha',u',\omega'))_+\rangle_{\mathcal{H}}\\&\qquad\equiv\Delta(u\boldsymbol{k}+u'\boldsymbol{k}')\Delta(u+u')\ \Delta(\omega+\omega')S^{ff}_{\alpha\alpha'}(\boldsymbol{k},u,\omega)\end{aligned}\tag{C1}$$

where

$$\begin{aligned}S^{ff}_{\alpha\alpha'}(\boldsymbol{k},u,\omega)=-\frac{1}{N}\sum_{\alpha_1\alpha_2}\sum_{\boldsymbol{q}_1\omega_1\sigma_1}&[V(\alpha_1,\boldsymbol{q}_1,\sigma_1,-)V(\alpha_2,\boldsymbol{q}_1,\sigma_1,+)/(\mathrm{i}\omega_1+\varepsilon(\boldsymbol{q}_1,\sigma_1))]\\&\times\langle(X(\alpha,u,\omega)X(\alpha',-u,-\omega)X(\alpha_1,u_1=-,-\omega_1)X(\alpha_2,u_2=+,\omega_1))_+\rangle_c.\end{aligned}\tag{C2}$$

In this equation there is a cumulant with four X-operators of the 'Fermi type'. This and the higher-order cumulants of X-operators are non-zero because of the correlations that are built into the ionic states, as the infinite Coulomb repulsion is hidden in the 'free-ion' Hamiltonian $\mathcal{H}_0$ of equation (2.4). The rules for calculating the cumulants appearing in rule 3.7 of I for the general model (cf. section 2 in I) are summarized in appendix B, but only the results for the PAM with $U=\infty$ are necessary, and in this case the expressions are simpler

because there are only two ionic transitions $\alpha = (0, \sigma)$. Assuming that H_h commutes with the σ-component of spin, and hence that there is conservation of σ in the GF, it follows that $\alpha = \alpha' = (0, \sigma)$ in equation (C2). The contribution of the graph in figure 4(c) is independent of $\boldsymbol{k}$, and employing a spin-independent hybridization $V(\boldsymbol{k}, \sigma) = V(\boldsymbol{k})$ it is given by

$$\begin{aligned} S^0_\sigma(\omega) = \frac{1}{N}\sum_{\boldsymbol{q}} |V(\boldsymbol{q})|^2 \{ & [D_\sigma(1-D_\sigma) - x_\sigma^2] K_\sigma(\omega)\beta I^0_{1,\sigma}(\boldsymbol{q}) \\ & - [D_\sigma(1-D_\sigma) + x_\sigma] K^2_\sigma(\omega) G^0_{\boldsymbol{q},\sigma}(\omega) \\ & - D_\sigma [K_\sigma(\omega) I^0_{2,\sigma}(\boldsymbol{q}) + K^2_\sigma(\omega) I^0_{1,\sigma}(\boldsymbol{q})]\} \end{aligned} \tag{C3}$$

where $x_\sigma = \langle X_{\sigma\sigma}\rangle$, $K_\sigma(\omega_s) = G^0_{f,\sigma}(\omega_s)/D_\sigma = -1/(\mathrm{i}\omega_s - \varepsilon_{f\sigma})$ and

$$I^0_{\ell,\sigma}(\boldsymbol{q}) = \frac{1}{\beta}\sum_{\omega_1} G^0_{\boldsymbol{q},\sigma}(\omega_1) K^\ell_\sigma(\omega_1) \qquad (\text{with } \ell = 1, 2). \tag{C4}$$

Employing the usual complex integration techniques [19, 22] one obtains for zero magnetic field

$$I^0_{1,\sigma}(\boldsymbol{q}) = (f_T(\varepsilon_{\boldsymbol{q}}) - f_T(\varepsilon_f))/(\varepsilon_{\boldsymbol{q}} - \varepsilon_f)$$

and

$$I^0_{2,\sigma}(\boldsymbol{q}) = (-f_T(\varepsilon_{\boldsymbol{q}}) + f_T(\varepsilon_f) + (\varepsilon_{\boldsymbol{q}} - \varepsilon_f) f'_T(\varepsilon_f))/(\varepsilon_{\boldsymbol{q}} - \varepsilon_f)^2$$

where $f_T(z) = (1 + \exp(z/T))^{-1}$ is the Fermi function and $f'_T(z)$ its derivative with respect to z.

To obtain $S^{CH}_\sigma(\boldsymbol{k}, \omega)$, note that in figure 4(b) there are infinitely many graphs with loops of any length. From equation (C3) it is then clear that $S^{CH}_\sigma(\boldsymbol{k}, \omega)$ is obtained by substituting for $G^0_{\boldsymbol{q},\sigma}(\omega)$ in equations (C3) and (C4) with the $G_{c,\sigma}(\boldsymbol{q}, \omega)$ (cf. equation (3.11)) represented by the diagrams in figure 1(c). When a local hybridization $V(\boldsymbol{k}) = V$ is considered, all of the $G_{c,\sigma}(\boldsymbol{q}, \omega)$ appear in equation (C3) only in the combination

$$(1/N)\sum_{\boldsymbol{q}} G_{c,\sigma}(\boldsymbol{q}, \omega) \equiv C_{c,\sigma}(\omega)$$

which was already obtained for a rectangular band of width $2W$ centred at the energy E_0 in section 4 (cf. equation (4.4)). The expression for $S^{CH}_\sigma(\mathrm{k}, \omega)$ is again independent of $\boldsymbol{k}$ and is given by

$$S^{CH}_\sigma(\boldsymbol{k}, \omega) = -|V|^2 \{A K_\sigma(\omega) + B K^2_\sigma(\omega) C_{c,\sigma}(\omega) + C K^2_\sigma(\omega)\} \tag{C5}$$

where $A = \left[D^0_\sigma(1 - D^0_\sigma) - x^2_\sigma\right]\beta I_1 - D^0_\sigma I_2$; $B = -D^0_\sigma(1 - D^0_\sigma) + x_\sigma$; and $C = -D^0_\sigma I_1$; and

$$I_\ell = \frac{1}{\beta}\sum_{\omega_1} C_{c,\sigma}(\omega_1) K^\ell_\sigma(\omega_1) \qquad (\text{with } \ell = 1, 2) \tag{C6}$$

and $K_\sigma(\omega_s) = -1/(\mathrm{i}\omega_s - \varepsilon_{f\sigma}) = G^0_{f,\sigma}(\omega_s)/D^0_\sigma$. This is the result shown in section 4.

References

[1] Hubbard J 1966 *Proc. R. Soc.* A **296** 82

[2] Hubbard J 1964 *Proc. R. Soc.* A **276** 238; 1964 *Proc. R. Soc.* A **277** 237; 1964 *Proc. R. Soc.* A **281** 401 These are the first three papers of a series of six.

[3] Figueira M S, Foglio M E and Martinez G G 1994 *Phys. Rev.* B **50** 17 933

[4] Wortis M 1974 *Phase Transitions and Critical Phenomena* vol 3, ed C Domb and M S Green (London: Academic) p 113
[5] Metzner W 1991 *Phys. Rev.* B **43** 8549
[6] Hewson A C 1977 *J. Phys. C: Solid State Phys.* **10** 4973
[7] Anda E V 1981 *J. Phys. C: Solid State Phys.* **14** L1037
[8] Figueira M S and Foglio M E 1994 *Physica* A **208** 279
[9] Baym G and Kadanoff L P 1961 *Phys. Rev.* **124** 287
Baym G 1962 *Phys. Rev.* **127** 1391
[10] Kubo R 1962 *J. Phys. Soc. Japan* **17** 1100
[11] Negele J W and Orland H 1988 *Quantum Many-Particle Systems* (New York: Addison-Wesley) ch 2
[12] Bloch C and Langer J S 1965 *J. Math. Phys* **6** 554
[13] Englert R 1963 *Phys. Rev.* **129** 567
[14] Figueira M S 1994 *Doctoral Thesis* Universidade Estadual de Campinas
[15] Foglio M E and Falicov L M 1979 *Phys. Rev.* B **20** 4554
[16] Gutzwiller M C 1965 *Phys. Rev* A **137** 1726
[17] Coleman P 1984 *Phys. Rev.* B **29** 3035
Newns D M and Read N 1987 *Adv. Phys.* **36** 799
[18] Foglio M E 1991 *Phys. Rev.* B **43** 3192
[19] Martinez Pino G G 1989 *Doctoral Thesis* Universidade Estadual de Campinas
[20] Gaudin M 1960 *J. Nucl. Phys.* **15** 89
[21] Yang D H Y and Wang Y L 1975 *Phys. Rev.* B **10** 4714
[22] Kadanoff L P and Baym G 1962 *Quantum Statistical Mechanics* (New York: Benjamin)